Novel 1,2,4-triazole clubbed with 1,3,4-oxadiazole motifs as efficient antimicrobial agents from N-arylsydnone as synthon

Shipa M Somagond[a], Ravindra R Kamble[a,*], Belgur S Sudha[b], Sheetal B Margankop[c], Pramod P Kattimani[d] & Shrinivas D Joshi[e]

[a]Department of Studies in Chemistry, Karnatak University Dharwad – 580 003, Karnataka, India

[b]Department of Chemistry, Yuvaraja's College, Mysore – 570 005, Karnataka, India

[c]Department of Chemistry, Government First Grade College, Paschapur -591 122, Karnataka, India

[d]Department of Chemistry, JSS Arts, Science and Commerce College, Gokak 591 307, Karnataka, India

[e]Novel Drug Design and Discovery Laboratory, Department of Pharmaceutical Chemistry, S.E.T.'s College of Pharmacy, Dharwad -580 002, Karnataka, India

*E-mail: ravichem@kud.ac.in

1,2,4-Triazoles and 1,3,4-oxadiazoles independently are very important pharmacophores. In view of this, a new class of 1,2,4-triazole clubbed with 1,3,4-oxadiazole motifs have been prepared and characterized by IR, ^{1}H NMR, ^{13}C NMR and mass spectral analysis. Molecular docking of all the title compounds into *S. aureus tyrosyl-tRNA synthetase* (PDB: 1JIJ) and *lanosterol 14α-demethylase* complex with standard inhibitor Fluconazole (PDB: 3KHM) is performed which snugly fitted into the active site thus explaining their excellent inhibitory activity exhibiting their possible antibacterial and antifungal activity, respectively. Drug-likeliness, Drug score values and toxicity prediction analyses of all the title compounds have shown favourable values and these molecules belong to Class 4 and Class 5 categories which make them useful scaffolds. Interestingly, the compounds **7h**, **7i**, **7k**, **7u** and **7v** have exhibited majestic antibacterial activity. Also, these compounds have shown antifungal activity against all pathogenic fungal strains with lower MIC value ranging from 0.50 - 4.00 µg/mL.

Keywords: 1,3,4-Oxadiazole, Anti-fungal activity, Anti-bacterial activity, 1, 2, 4-Triazole

Heteroaromatic ring systems are the key moieties in drug molecules that are generally used since they resemble the biologically active compounds within our body such as the nucleic acids, neurotransmitters and hormones etc. Among the several heteroaromatic rings at hand, oxadiazole is one in all the necessary rings of the many pharmaceutical products. Depending on the position of the nitrogen and oxygen the isomers of oxadiazoles are 1,3,4-oxadiazole, 1,2,5-oxadiazole, 1,2,3-oxadiazole, 1,2,4-oxadiazole as shown in below Fig. 1.[1] Among these, 1,3,4-oxadiazole is wide studied as a result of its extensive pertinence in research [2] and its demonstration of therapeutic activities.

1,3,4-Oxadiazole is a derivative of furan in which two =CH have been replaced with two nitrogen atoms due to which the aromaticity of the ring is reduced and thus resulted 1,3,4-oxadiazole ring still exhibits conjugated diene character[3]. The toxophoric –N=C–O– linkage present in 1,3,4-oxadiazole leads to a significant pharmacological properties such as

antitumor[4], hypoglycemic, antipyretic[5], anti-viral[6], anti-inflammatory[7], insecticidal[8], CNS stimulant, anti-amoebic, antiemetic, antidepressant, anthelmintic vasodilator, anti-mycotic activities etc [9]. 1,3,4-Oxadiazole is an important moiety in the commercially available drugs (Fig. 2) such as Raltegravir (antiviral), Nesapidil (anti-arrhythmic), and Furamizole (potent antibacterial)[10], Zibotentan (anticancer)[11], and Tiodazosin anti-hypertensive[12].

Triazoles have shown to possess a variety of fascinating features within the framework of medicinal chemistry. They are stable to acidic/basic reaction and conjointly reductive/oxidative conditions, investigative of a high aromatic stabilization and this scaffold is comparatively resistant to metabolic

1,3,4-Oxadiazole   1,2,5-Oxadiazole   1,2,3-Oxadiazole   1,2,4-Oxadiazole
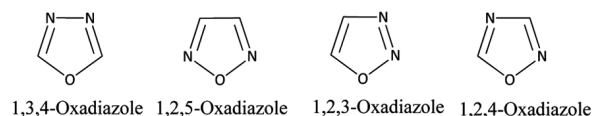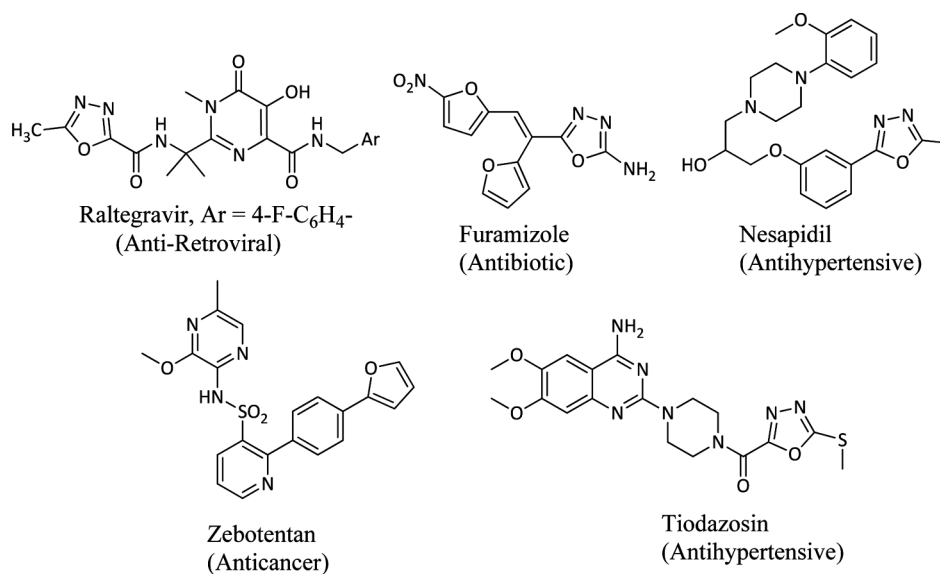
Fig. 1 — Isomers of oxadiazoles

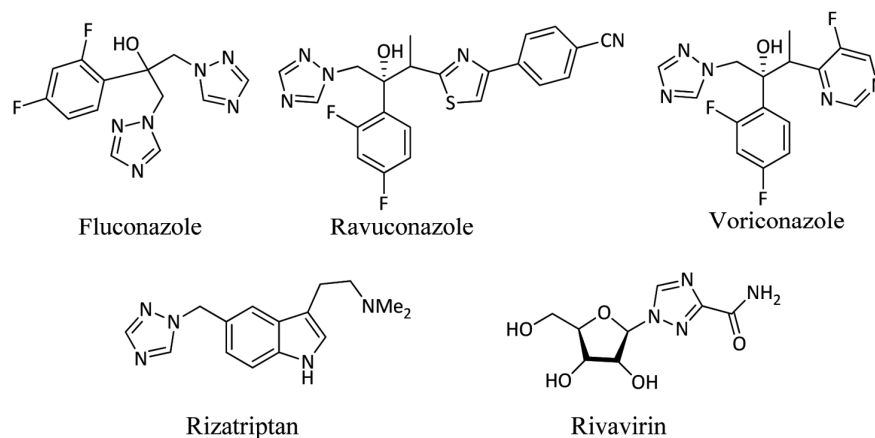Fig. 2 — Commercially available drugs containing 1,3,4-oxadiazole nucleus

Fig. 3 — Marketed drugs containing 1,2,4-triazole ring

degradation. The diverse pharmacological properties of 1,2,4- triazoles as antifungal, antiviral, herbicidal, and *catalase* inhibitors induced deep interest to discover new entities for their broader applications. Most of the existing antifungal drugs hold 1,2,4-triazole pharmacophore in their elemental structures which proves the antifungal potencies of the 1,2,4-triazole template so that it expresses significant antimicrobial activity [13]. There are drugs in clinical use for various ailments which have 1,2,4-triazole as core moiety *e.g.*, Fluconazole, Ravuconazole, Voriconzole (all antifungal), Rizatriptan (antimigraine), Rivavirin (antiviral) as shown in Fig. 3[14].

N-arylsydnone act as functional and a useful synthon for the synthesis of various biologically

Fig. 4 — Structure of the 1,2,4-triazole clubbed 1,3,4-oxadiazoles

active heterocycles *viz*., pyrazoles, 1,3,4-oxadiazoles, phenyl indazoles, pyrazolines, and tetrazines *via* 1,3-dipolar cycloaddition and addition elimination reactions[15]. In view of the above observations 1,2,4-triazole **2a-b** was prepared using N-arylsydnone and further appended to the 1,3,4-oxadiazole as shown in Fig. 4 in order to explore the possible antibacterial as well as antifungal propensity after computationally analyzing the inhibition of the enzymes *tyrosyl-tRNA synthetase*[16] (PDB: 1JIJ,

for antibacterial property) and *lanosterol 14α-demethylase* (PDB:3KHM), for the antifungal property)[17]. Also, the molecular weight, hydrogen bond donors/acceptors (HBD/HBA), permeation (logP), polar surface area (TPSA), solubility limit (logS), and as a result drug likeliness and drug score have been predicted. The toxicity viz., carcinogenicity, immunogenicity, mutagenicity, cytotoxicity, tumorigenicity, hepatotoxicity of the title compounds in comparison with the standard drugs used during *in vitro* antimicrobial assessment have been predicted.

Results and Discussion

Chemistry

The reaction sequences working for the synthesis of compounds **7g-p** and **9t-y** are outlined in the Scheme 1. *N*-arylsydnone **1a-b** was ring transformed to 3-aryl-5-methyl-1,3,4-oxadiazol-2(3*H*)-one upon bromination at 0 ºC followed by heating at 70ºC in presence of acetic anhydride *via* [3+2] cycloaddition and further refluxed with formamide at 180ºC. This resulted into the ring insertion of nitrogen and demethylation at C_5 forming 2-aryl-2*H*-1,2,4-triazol-

3(4*H*)-one **2a-b**[18]. Further, we successfully explored **2a-b** for the synthesis of various Schiff bases and fused heterocyclic compounds which are depicted in Scheme 1. 2-Aryl-2*H*-1,2,4-triazol-3(4*H*)-one **2a-b** underwent *N*-alkylation on reaction with ethylbromoacetate in presence of sodium ethoxide under reflux to yield the ester **3a-b** which was further heated with hydrazine hydrate (99%) to get the corresponding acid hydrazide **4a-b**. The newly synthesized 2-(5-oxo-1-aryl-1*H*-1,2,4-triazol-4(5*H*)-yl)acetohydrazide **4a-b** was condensed with aromatic aldehydes **5c-f** in acetic acid followed by neutralization with ammonia solution resulted into Schiff bases **6g-p**. These Schiff bases **6g-p** were further treated with Ac₂O which cyclize to 1,2,4-triazole clubbed 4,5-dihydro-1,3,4-oxadiazoles **7g-p**. On the other hand **4a-b** was also cyclized to 1,2,4-triazole appended to 1,3,4-oxadiazoles **9t-y** when treated with aromatic carboxylic acid **8q-s** in the presence of POCl₃ [19].

Structures of all the newly synthesized compounds **7g-p** and **9t-y** were confirmed by spectral characterization. FT-IR spectral analysis of the
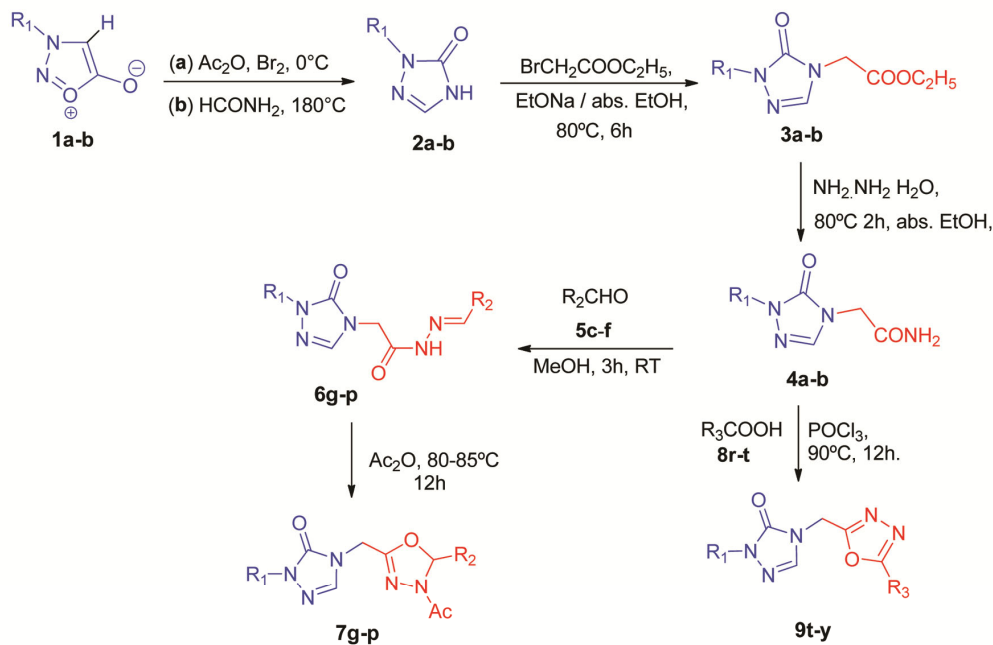
a; R₁ = C₆H₅ **b**; R₁ = C₆H₅ **c;** R₂ = C₆H₅ **d)** R₂ = 4-NO₂-C₆H₄; **e)** R₂ = 4-Cl-C₆H₄ **f**; R₂ = 4-F-C₆H₄ **g;** R₁ = C₆H₅, R₂ = C₆H₅ **h**; R₁ = C₆H₅, R₂ = 4-NO₂-C₆H₄ **i**; R₁ = C₆H₅, R₂ = 4-Cl-C₆H₄ **j**; R₁ = C₆H₅, R₂ = 4-F-C₆H₄ **k)** R₁ = C₆H₅, R₂ = 4-CH₃O-C₆H₄ **l**; R₁ = 4-CH₃O-C₆H₄, R₂ = C₆H₅ **m;** R₁ = 4-CH₃O-C₆H₄, R₂ = 4-NO₂-C₆H₄ **n**; R₁ = 4-CH₃O-C₆H₄, R₂ = 4-Cl-C₆H₄ **o**; R₁ = 4-CH₃O-C₆H₄, R₂ = 4-F-C₆H₄ **p**; R₁ = 4-CH₃O-C₆H₄, R₂ = 4-CH₃O-C₆H₅ **q**; R₃ = C₆H₅, **r;** R₃ = 4-NO₂-C₆H₄ **s**; R₃ = 4-Cl-C₆H₄ **t**; R₁ = C₆H₅, R₃ = C₆H₅ **u;** R₁ = C₆H₅, R₃ = 4-NO₂-C₆H₄ **v**; R₁ = C₆H₅, R₃ = 4-Cl-C₆H₅ w; R₁ = 4-CH₃O-C₆H₄, R₃ = C₆H₅ **x**; R₁ = 4-CH₃O-C₆H₄, R₃ = 4-NO₂-C₆H₄ **y**; R₁ = 4-CH₃O-C₆H₄, R₃ = 4-Cl-C₆H₄

Scheme 1 — Synthetic route for the synthesis of compounds **7g-p** and **9t-y**

compounds **7g-p** and **9t-y** exhibited a sharp intense band around 1700-1720 cm^{-1} due to C=O stretching frequency of the triazole. The sharp band for C=N appeared in the range 1600-1670 cm^{-1}. ^{1}H NMR spectra of these compounds displayed a singlet in the range 4.50-4.99 ppm for N-CH$_2$ protons. ^{1}H NMR spectra of compounds **9t-y** displayed a singlet in the range 5.30-5.70 ppm for N-CH$_2$ protons. ^{13}C NMR spectrum indicated that all the title compounds exhibited the number of signals equivalent to the magnetically non equivalent carbon atoms. The mass spectrum of **7g-p** and **9t-y** revealed that observed molecular ion peaks were in good agreement with molecular mass and were further confirmed using CHN analysis.

Experimental Section

Melting points (mp) were determined using the Thomas Hoover automated melting point apparatus and are uncorrected. ^{1}H NMR at 400 MHz and ^{13}C NMR at 100 MHz were recorded using a Jeol ECX spectrometer. All the chemical shifts were referenced to TMS as internal standard reference. The shifts were reported in ppm with delta scale (δ). Infrared spectral (IR) data were determined using Perkin Elmer FT-IR spectrophotometer. Shimadzu GCMS – TQ8050 Mass spectrometer was used to record molecular masses of the compounds. Commercial reagents and analytical grade solvents used for the reaction, analyses were directly used without purification. The chemicals and solvents used were purchased from Alfa Aesar, Sigma Aldrich, TCI Chemicals and Spectrochem. Reaction progress was monitored on thin layer chromatography sheets i.e. (TLC) of Merck Kiesel 60 F254 of 0.2 mm sheets. Spot of intermediates and final compounds monitored on TLC were visualized on UV-lamp, iodine stain. The starting compounds **1-4a-b** and **6g-p** were prepared according to the reported methods[18].

Synthesis and characterization of compounds

General procedure for the synthesis of 4-((4-acetyl-5-aryl-4,5-dihydro-1,3,4-oxadiazol-2-yl)methyl)-2-aryl-2*H*-1,2,4-triazol-3(4*H*)-one, 7g-p

A solution of (*E*)-*N'*-(4-sustituted-benzylidene)-2-(5-oxo-1-aryl-1*H*-1,2,4-triazol-4(5*H*)-yl)acetohydrazide **6g-p** (10 mmol) in acetic anhydride (25 ml) was heated to 80-85 ºC for 12h. The reaction was monitored by TLC. After completion of the reaction, reaction mixture was cooled to 25-30ºC and quenched to ice cold water and extracted the compound into ethyl acetate. The ethyl acetate was distilled under

reduced pressure to get crude product which was purified by column chromatography to obtain 4-((4-acetyl-5-aryl-4,5-dihydro-1,3,4-oxadiazol-2-yl) methyl)-2-aryl-2*H*-1,2,4-triazol-3(4*H*)-one (**7g-p**). The IR, mass and NMR spectra of the compounds are shown in Figs S1-S8 in Supplementary Information.

4-((4-Acetyl-5-phenyl-4,5-dihydro-1,3,4-oxadiazol-2-yl)methyl)-2-phenyl-2*H*-1,2,4-triazol-3(4*H*)-one, 7g: Brown (Yield: 60%), mp: 104-106ºC; IR (KBr, cm^{-1}): 1710 (C=O), 1666 (C=O), 1665 (C=N), 1082 (C-N); ^{1}H NMR (400 MHz, DMSO-*d$_6$*) δ (ppm): 2.40 (s, 3H CH$_3$), 4.49 (s, 2H, CH$_2$), 6.81 (s, 1H, CH, oxadiazole), 7.12-8.23 (m, 10H, Ar-H), 8.23 (s, 1H, triazole); ^{13}C NMR (100 MHz, DMSO-*d$_6$*) δ (ppm): 21.80, 44.93, 78.14, 119.08, 125.79, 129.08, 131.92, 133.75, 135.80, 139.53, 144.04,151.09, 156.76, 169.22, 172.07; MS (70 eV) *m/z*: 363 [M$^+$]; CHN analysis for C$_{19}$H$_{17}$N$_5$O$_3$ (%): Calcd: C 62.80; H 4.72; N 19.27; Found: C 62.92; H 4.79; N 19.36.

4-((4-Acetyl-5-(4-nitrophenyl)-4,5-dihydro-1,3,4-oxadiazol-2-yl)methyl)-2-phenyl-2*H*-1,2,4-triazol-3(4*H*)-one, 7h: Brown (Yield: 72%), mp: 198-200ºC; IR (KBr, cm^{-1}): 1706 (C=O), 1670 (C=O), 1661 (C=N), 1086 (C-N); ^{1}H NMR (400 MHz, DMSO-*d$_6$*) δ (ppm): 2.43 (s, 3H CH$_3$), 4.43 (s, 2H, CH$_2$), 6.92 (s, 1H, CH, oxadiazole), 7.17-8.14 (m, 9H, Ar-H), 8.25 (s, 1H, triazole); ^{13}C NMR (100 MHz, DMSO-*d$_6$*) δ (ppm): 21.09, 43.92, 79.34, 118.82, 125.92, 129.09, 132.09, 133.86, 135.09, 138.05, 147.05, 151.86, 156.82, 169.72, 172.01; MS (70 eV) *m/z*: 408 [M$^+$]; CHN analysis for C$_{19}$H$_{16}$N$_6$O$_5$ (%): Calcd: C 55.88; H 3.95; N 20.58; Found: C 55.91; H 3.99; N 20.64.

4-((4-Acetyl-5-(4-chlorophenyl)-4,5-dihydro-1,3,4-oxadiazol-2-yl)methyl)-2-phenyl-2*H*-1,2,4-triazol-3(4*H*)-one, 7i: Pale yellow (Yield: 67%), mp: 132-134ºC; IR (KBr, cm^{-1}): 1708 (C=O), 1675 (C=O), 1653 (C=N), 1088 (C-N); ^{1}H NMR (400 MHz, DMSO-*d$_6$*) δ (ppm): 2.42 (s, 3H CH$_3$), 4.52 (s, 2H, CH$_2$), 6.90 (s, 1H, CH, oxadiazole), 7.18-8.21 (m, 9H, Ar-H), 8.25 (s, 1H, triazole); ^{13}C NMR (100 MHz, DMSO-*d$_6$*) δ (ppm): 21.56, 43.73, 79.04, 118.35, 125.81, 129.68, 131.72, 133.15, 135.30, 139.13, 145.39, 151.56, 156.57, 169.59, 172.71; MS (70 eV) *m/z* (Spectrum No. 2): 399 [M+2], 397 [M$^+$]; CHN analysis for C$_{19}$H$_{16}$ClN$_5$O$_3$ (%): Calcd: C 57.36; H 4.05; N 17.60; Found: C, 57.42; H, 4.12; N, 17.69.

4-((4-Acetyl-5-(4-fluorophenyl)-4,5-dihydro-1,3,4-oxadiazol-2-yl)methyl)-2-phenyl-2*H*-1,2,4-triazol-3(4*H*)-one, 7j: Brown (Yield: 60%), mp: 240-242ºC; IR (KBr, cm^{-1}): 1715 (C=O), 1665 (C=O), 1645 (C=N), 1086 (C-N); ^{1}H NMR (400 MHz,

DMSO-d_6) δ (ppm): 2.42 (s, 3H CH$_3$), 4.41 (s, 2H, CH$_2$), 6.87 (s, 1H, CH, oxadiazole), 7.12-8.20 (m, 9H, Ar-H), 8.24 (s, 1H, triazole); ^{13}C NMR (100 MHz, DMSO-d_6) δ (ppm): 21.36, 44.23, 79.34, 118.73, 125.78, 129.82, 131.67, 133.29, 135.76, 139.52, 142.87, 152.06, 156.81, 169.09, 172.10; MS (70 eV) *m/z*: 381 [M $^+$]; CHN analysis for C$_{19}$H$_{16}$FN$_5$O$_3$ (%): Calcd: C, 59.84; H, 4.23; N, 18.36; Found: C, 59.89; H, 4.28; N, 18.41.

4-((4-Acetyl-5-(4-methoxyphenyl)-4,5-dihydro-1,3,4-oxadiazol-2-yl)methyl)-2-phenyl-2*H*-1,2,4-triazol-3(4*H*)-one, 7k: Brown (Yield: 65%), mp: 123-125°C; IR (KBr, cm^{-1}): 1707 (C=O), 1672 (C=O), 1670 (C=N), 1089 (C-N); ^{1}H NMR (400 MHz, DMSO-d_6) δ (ppm): 2.04 (s, 3H CH$_3$), 3.72 (s, 3H, OCH$_3$), 4.41 (s, 2H, CH$_2$), 6.98 (s, 1H, CH, oxadiazole), 7.00-8.12 (m, 9H, Ar-H), 8.25 (s, 1H, triazole); ^{13}C NMR (100 MHz, DMSO-d_6) δ (ppm): 21.32, 42.18, 55.73, 90.13, 114.23, 120.69, 123.88, 127.42, 134.16, 138.81, 144.21, 148.24, 152.08, 156.09, 167.31, 169.49; MS (70 eV) *m/z*: 393 [M$^+$]; CHN analysis for C$_{20}$H$_{19}$N$_5$O$_4$ (%): Calcd: C, 61.06; H, 4.87; N, 17.80; Found: C, 61.17; H, 4.91; N, 17.84.

4-((4-Acetyl-5-phenyl-4,5-dihydro-1,3,4-oxadiazol-2-yl)methyl)-2-(4-methoxyphenyl)-2*H*-1,2,4-triazol-3(4*H*)-one, 7l: Brown (Yield: 75%), mp: 257-259°C; IR (KBr, cm^{-1}): 1710 (C=O), 1675 (C=O), 1658 (C=N), 1088 (C-N); ^{1}H NMR (400 MHz, DMSO-d_6) δ (ppm): 2.48 (s, 3H CH$_3$), 3.75 (s, 3H, OCH$_3$), 4.41 (s, 2H, CH$_2$), 6.91 (s, 1H, CH, oxadiazole), 7.12-8.18 (m, 9H, Ar-H), 8.25 (s, 1H, triazole); ^{13}C NMR (100 MHz, DMSO-d_6) δ (ppm): 21.34, 42.16, 55.75, 90.02, 114.33, 120.72, 123.90, 127.92, 134.26, 138.76, 143.61, 148.78, 151.38, 156.54, 167.43, 169.27; MS (70 eV) *m/z*: 393 [M$^+$]; CHN analysis for C$_{20}$H$_{19}$N$_5$O$_4$ (%): Calcd: C, 61.06; H, 4.87; N, 17.80; Found: C, 61.17; H, 4.91; N, 17.84.

4-((4-Acetyl-5-(4-nitrophenyl)-4,5-dihydro-1,3,4-oxadiazol-2-yl)methyl)-2-(4-methoxyphenyl)-2*H*-1,2,4-triazol-3(4*H*)-one, 7m: Brown (Yield: 67%), mp: 147-149°C; IR (KBr, cm^{-1}): 1705 (C=O), 1665 (C=O), 1083 (C-N); ^{1}H NMR (400 MHz, DMSO-d_6) δ (ppm): 2.46 (s, 3H CH$_3$), 3.72 (s, 3H, OCH$_3$), 4.42 (s, 2H, CH$_2$), 7.00 (s, 1H, CH, oxadiazole), 7.14-8.12 (m, 8H, Ar-H), 8.25 (s, 1H, triazole); ^{13}C NMR (100 MHz, DMSO-d_6) δ (ppm): 21.55, 43.56, 55.79, 90.19, 114.73, 120.34, 124.50, 128.59, 131.36, 138.56, 143.54, 148.73, 151.46, 156.70, 167.26, 169.67; MS (70 eV) *m/z*: 438 [M $^+$]; CHN analysis for C$_{20}$H$_{18}$N$_6$O$_6$ (%): Calcd: C, 54.79; H, 4.14; N, 19.17; Found: C, 54.81; H, 4.19; N, 19.22.

4-((4-Acetyl-5-(4-chlorophenyl)-4,5-dihydro-1,3,4-oxadiazol-2-yl)methyl)-2-(4-methoxyphenyl)-2*H*-1,2,4-triazol-3(4*H*)-one, 7n: Pale yellow (Yield: 75%), mp: 122-124°C; IR (KBr, cm^{-1}): 1718 (C=O), 1667 (C=O), 1646 (C=N), 1087 (C-N); ^{1}H NMR (400 MHz, DMSO-d_6) δ (ppm): 2.48 (s, 3H CH$_3$), 3.78 (s, 3H, OCH$_3$), 4.46 (s, 2H, CH$_2$), 7.09 (s, 1H, CH, oxadiazole), 7.18-8.19 (m, 8H, Ar-H), 8.25 (s, 1H, triazole); ^{13}C NMR (100 MHz, DMSO-d_6) δ (ppm): 21.54, 43.09, 55.75, 90.01, 115.81, 120.52, 125.81, 129.07, 131.09, 138.06, 143.21, 148.99, 152.06, 156.55, 167.69, 169.84; MS (70eV) *m/z*: 429[M + 2], 427 [M $^+$]; CHN analysis for C$_{20}$H$_{18}$N$_5$ClO$_4$ (%): Calcd: C, 56.15; H, 4.24; N, 16.37; Found: C, 56.21; H, 4.31; N, 16.42.

4-((4-Acetyl-5-(4-fluorophenyl)-4,5-dihydro-1,3,4-oxadiazol-2-yl)methyl)-2-(4-methoxyphenyl)-2*H*-1,2,4-triazol-3(4*H*)-one, 7o: Brown (Yield: 62%), mp: 145-147°C; IR (KBr, cm^{-1}): 1705 (C=O), 1668 (C=O), 1642 (C=N), 1083 (C-N); ^{1}H NMR (400 MHz, DMSO-d_6) δ (ppm): 2.43 (s, 3H, CH$_3$), 3.70 (s, 3H, OCH$_3$), 4.46 (s, 2H, CH$_2$), 7.03 (s, 1H, CH, oxadiazole), 7.17-8.18 (m, 8H, Ar-H), 8.25 (s, 1H, triazole); ^{13}C NMR (100 MHz, DMSO-d_6) δ (ppm): 21.53, 43.57, 55.70, 90.30, 114.63, 120.68, 124.81, 128.29, 131.46, 138.86, 143.91, 148.20, 151.89, 156.76, 167.08, 169.82; MS (70 eV) *m/z*: 411 [M $^+$]; CHN analysis for C$_{20}$H$_{18}$N$_5$FO$_4$ (%): Calcd: C 58.39; H, 4.41; N, 17.02; Found: C, 58.43; H, 4.48; N, 17.13.

4-((4-Acetyl-5-(4-methoxyphenyl)-4,5-dihydro-1,3,4-oxadiazol-2-yl)methyl)-2-(4-methoxyphenyl)-2*H*-1,2,4-triazol-3(4*H*)-one, 7p: Brown (Yield: 59%), mp: 170-172°C; IR (KBr, cm^{-1}): 1701 (C=O), 1663 (C=O), 1647 (C=N), 1084 (C-N); ^{1}H NMR (400 MHz, DMSO-d_6) δ (ppm): 2.48 (s, 3H CH$_3$), 3.77 (s, 3H, OCH$_3$), 4.48 (s, 2H, CH$_2$), 7.02 (s, 1H, CH, oxadiazole), 7.17-8.10 (m, 8H, Ar-H), 8.24 (s, 1H, triazole); ^{13}C NMR (100 MHz, DMSO-d_6) δ (ppm): 21.41, 43.33, 55.75, 90.02, 114.41, 120.43, 124.65, 128.06, 132.56, 137.06, 144.64, 149.03, 152.36, 156.75, 167.36, 169.17; MS (70 eV) *m/z*: 423 [M $^+$]; CHN analysis for C$_{21}$H$_{21}$N$_5$O$_5$ (%): Calcd: C, 59.57; H, 5.00; N, 16.54; Found: C, 59.69; H, 5.09; N, 16.58.

General procedure for the synthesis of 2-(4-aryl)-4-((5-phenyl-1,3,4-oxadiazol-2-yl)methyl)-2*H*-1,2,4-triazol-3(4*H*)-one, 9t-y

A mixture of 2-(5-oxo-1-aryl-1*H*-1,2,4-triazol-4(5*H*)-yl)acetohydrazide **4a-b** (1.00 mmol) and substituted benzoic acids **8q-s** (1.00 mmol) in phosphorus oxychloride (2.00 mL) was refluxed on

water bath for 9 h. The progress of the reaction was monitored by TLC using Toluene: Ethylacetate: Methanol (70:20:10) as eluents. After the completion of reaction, it was cooled and poured onto crushed ice with continuous stirring. The solid thus obtained was neutralized with sodium bicarbonate solution (10% w/v). The resulting solid thus obtained was collected by filtration, washed well with cold water, dried, and recrystallized from absolute ethanol to get another set of compounds **9t-y**. The IR, mass and NMR spectra of the compounds are shown in Figs S9-S17 in Supplementary Information.

2-Phenyl-4-((5-phenyl-1,3,4-oxadiazol-2-yl) methyl)-2*H*-1,2,4-triazol-3(4*H*)-one, 9t: White (Yield: 89%), mp: 216-218ºC; IR (KBr, cm^{-1}): 1714 (C=O), 1596 (C=N), 1558 (C=N); ^{1}H NMR (400 MHz, DMSO-d_6) δ (ppm): 5.43 (s, 2H, CH$_2$), 7.52-8.21 (m, 11H, Ar-H), 8.29 (s, 1H, triazole); ^{13}C NMR (100 MHz, DMSO-d_6) δ (ppm): 47.23, 118.56, 127.09, 127.13, 127.46, 128.03, 129.92, 130.06, 137.81, 146.32, 154.07, 163.58, 164.31; MS (70 eV) *m/z*: 319 [M$^+$]; CHN analysis for C$_{17}$H$_{13}$N$_5$O$_2$ (%): C, 63.94; H, 4.10; N, 21.93 Found: C, 63.97; H, 4.42; N, 21.99.

4-((5-(4-Nitrophenyl)-1,3,4-oxadiazol-2-yl) methyl)-2-phenyl-2*H*-1,2,4-triazol-3(4*H*)-one, 9u: White shiny solid (Yield: 91%), mp: 120-124ºC; IR (KBr, cm^{-1}): 1705 (C=O), 1675 (C=N), 1599 (C=N); ^{1}H NMR (400 MHz, DMSO-d_6) δ (ppm): 5.37 (s, 2H, CH$_2$), 7.22-8.41 (m, 9H, Ar-H), 8.43 (s, 1H, triazole); ^{13}C NMR (100 MHz, DMSO-d_6) δ (ppm): 42.70, 117.88, 124.63, 125.14, 128.01, 129.10, 137.45, 138.70, 149.30, 150.63, 162.76, 163.80, 165.65; LCMS (70 eV) *m/z*: 364 [M$^+$]; CHN analysis for C$_{17}$H$_{12}$N$_6$O$_4$ (%): C, 56.05; H, 3.32; N, 23.07 Found: C, 56.31; H, 3.47; N 23.13.

4-((5-(4-Chlorophenyl)-1,3,4-oxadiazol-2-yl) methyl)-2-phenyl-2*H*-1,2,4-triazol-3(4*H*)-one, 9v: White shiny solid (Yield: 88%), mp: 285-287ºC; IR (KBr, cm^{-1}): 1719 (C=O), 1672 (C=N), 1599 (C=N); ^{1}H NMR (400 MHz, DMSO-d_6) δ (ppm): 5.83 (s, 2H, CH$_2$), 6.99-8.15 (m, 9H, Ar-H), 8.18 (s, 1H, triazole); ^{13}C NMR (100 MHz, DMSO-d_6) δ (ppm): 48.54, 118.32, 123.14, 125.05, 127.30, 128.21, 128.15, 136.46, 139.70, 146.18, 154.09, 163.53, 164.59; MS (70 eV) *m/z*: 355 [M+2], 353[M$^+$]; CHN analysis for C$_{17}$H$_{12}$ClN$_5$O$_2$ (%): C, 57.72; H, 3.42; N, 19.80 Found: C, 57.81; H, 3.49; N, 19.87.

2-(4-Methoxyphenyl)-4-((5-phenyl-1,3,4-oxadiazol-2-yl)methyl)-2*H*-1,2,4-triazol-3(4*H*)-one, 9w: White shiny solid (Yield: 93%), mp: 177-179ºC; IR (KBr, cm^{-1}): 1705 (C=O), 1627 (C=N), 1561

(C=N); ^{1}H NMR (400 MHz, DMSO-d_6) δ (ppm): 3.45 (s, 3H, OCH$_3$), 5.55 (s, 2H, CH$_2$), 7.28-8.45 (m, 10H, Ar-H), 8.23 (s, 1H, triazole); ^{13}C NMR (100 MHz, DMSO-d_6) δ (ppm): 45.05, 55.61, 114.64, 120.34, 124.14, 126.23, 131.20, 134.68, 138.00, 142.42, 146.43, 163.01, 167.09, 169.03; MS (70 eV) *m/z*: 349 [M$^+$]; CHN analysis for C$_{18}$H$_{15}$N$_5$O$_3$ (%): C, 61.89; H, 4.33; N, 20.05 Found: C, 61.93; H, 4.47; N, 20.81.

2-(4-Methoxyphenyl)-4-((5-(4-nitrophenyl)-1,3,4-oxadiazol-2-yl)methyl)-2*H*-1,2,4-triazol-3(4*H*)-one, 9x: White shiny solid (Yield: 84%), mp: 234-236ºC; IR (KBr, cm^{-1}): 1715 (C=O), 1679 (C=N), 1609 (C=N); ^{1}H NMR (400 MHz, DMSO-d_6) δ (ppm): 3.62 (s, 3H, OCH$_3$), 5.32 (s, 2H, CH$_2$), 7.09-8.22 (m, 8H, Ar-H), 8.56 (s, 1H, triazole); ^{13}C NMR (100 MHz, DMSO-d_6): δ ppm 47.42, 55.91, 114.37, 114.72, 123.59, 125.01, 128.56, 130.38, 137.32, 145.29, 145.34, 154.19, 157.31, 163.29; MS (70 eV) *m/z*: 394 [M$^+$]; CHN analysis for C$_{18}$H$_{14}$N$_6$O$_5$ (%): C, 54.82; H, 3.58; N, 21.31 Found: C, 54.89; H, 3.67; N, 21.56.

4-((5-(4-Chlorophenyl)-1,3,4-oxadiazol-2-yl)methyl)-2-(4-methoxyphenyl)-2*H*-1,2,4-triazol-3(4*H*)-one, 9y: White (Yield: 89%), mp: 110-112ºC; IR (KBr cm^{-1}): 1745 (C=O), 1667 (C=N), 1592 (C=N); ^{1}H NMR (400 MHz, DMSO-d_6) δ (ppm): 3.53 (s, 3H, OCH$_3$), 5.29 (s, 2H, CH$_2$), 7.05-8.17 (m, 8H, Ar-H), 8.52 (s, 1H, triazole); ^{13}C NMR (100 MHz, DMSO-d_6) δ (ppm): 49.40, 55.42, 114.29, 122.31, 128.72, 128.83, 129.36, 135.52, 136.13, 145.01, 153.79, 156.52, 162.56, 163.51; MS *m/z* (70 eV): 385 [M+2], 383 [M$^+$]; CHN analysis for C$_{18}$H$_{14}$N$_5$ClO$_3$ (%): C, 56.33; H, 3.68; N, 18.25 Found: C, 56.45; H, 3.74; N, 18.44.

Pharmacological evaluation

Docking studies

Molecular docking gives an idea about the behaviour of small molecules in the building pocket of target proteins. The docking strategies lead to the druggability of the compounds and their specificity against particular target can be analyzed for further lead optimization process[20]. In this regard molecular docking was carried to clarify the binding mode of the compounds to provide the straightforward information for further structural optimization.

Docking against *S. aureus TyrRS* in complex with SB-239629 (PDB ID: 1JIJ)

The crystal structure of *S. aureus TyrRS* in complex with SB-239629 (PDB ID: 1JIJ, 3.20 Å X-ray

diffraction) was extracted from the Brookhaven Protein Database (PDB http://www.rcsb.org/pdb). The proteins were prepared for docking by adding polar hydrogen atom with Gasteiger-Huckel charges and water molecules were removed. The 3D structure of the ligands was generated by the SKETCH module implemented in the SYBYL program (Tripos Inc., St. Louis, USA) and its energy-minimized conformation was obtained with the help of the Tripos force field using Gasteiger-Huckel charges and molecular docking was performed with Surflex-Dock program that is interfaced with Sybyl-X 2.0 and other miscellaneous parameters were assigned with the default values given by the software[20].

To investigate the mechanism of antibacterial activity and detailed intermolecular interactions between the synthesized compounds, molecular docking studies were performed on the crystal structure of *S. aureus TyrRS* in complex with SB-239629 [21] using the surflex-dock program of sybyl-X 2.0 software. The predicted binding energies of the compounds are listed in Table 1. Docking study revealed that all the compounds showed very good docking score against the enzyme. Fig. 5 presents the compound **7m** making two hydrogen bonding
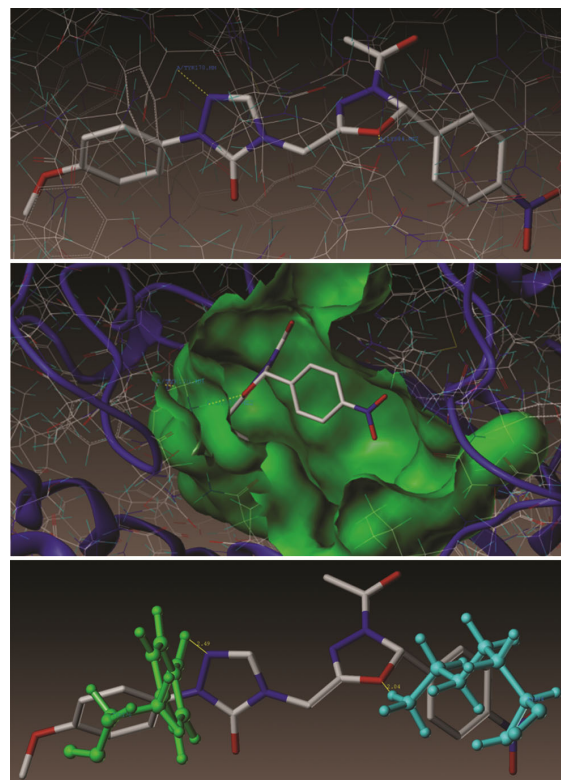

Fig. 5 — Docked view of compound **7m** at the active site of the enzyme PDB: 1JIJ

Table 1 — Surflex Docking score (kcal/mol) with *S. aureus* TyrRS in complex with SB-239629 (PDB ID: 1JIJ)

Entry No.	CScore[a]	Crash Score[b]	Polar Score[c]	D Score[d]	PMF Score[e]	G Score[f]	Chem Score[g]
7g	5.65	-2.15	2.54	-130.06	-18.73	-226.38	-22.70
7h	4.72	-0.30	1.09	-101.31	-47.04	-146.83	-12.56
7i	4.63	-0.31	1.70	-92.21	-44.67	-154.06	-13.93
7j	5.77	-1.46	2.40	-138.22	-35.38	-218.82	-20.74
7k	4.80	-1.01	0.01	-140.81	-39.20	-216.99	-15.97
7l	5.78	-0.58	1.78	-110.62	-56.61	-180.77	-17.01
7m	5.56	-2.11	1.31	-148.13	-73.84	-226.09	-17.58
7n	5.88	-0.73	3.33	-114.71	-71.74	-164.49	-17.76
7o	6.03	-3.18	2.30	-147.77	-18.27	-208.70	-21.81
7p	5.30	-1.44	2.43	-131.62	-77.08	-208.46	-20.05
9t	5.47	-1.01	0.91	-129.16	20.66	-208.56	-19.80
9u	5.69	-1.66	2.59	-131.95	-39.99	-217.23	-20.70
9v	4.69	-0.94	1.01	-95.37	-22.97	-161.41	-15.76
9w	5.24	-0.36	1.04	-118.07	-10.95	-172.67	-18.39
9x	5.96	-2.11	2.49	-137.14	-37.24	-209.06	-18.90
9y	5.40	-0.51	1.89	-102.41	-33.01	-160.28	-18.06
Tetracycline	3.57	-3.36	3.98	-117.83	-68.89	-132.01	-17.62

[a] CScore (Consensus Score) integrates a number of popular scoring functions for ranking the affinity of ligands bound to the active site of a receptor and reports the output of total score. [b] Crash-score revealing the inappropriate penetration into the binding site. Crash scores close to 0 are favorable. Negative numbers indicate penetration
[c] Polar indicating the contribution of the polar interactions to the total score. The polar score may be useful for excluding docking results that make no hydrogen bonds
[d] D-score for charge and van der Waals interactions between the protein and the ligand. [e] PMF-score indicating the Helmholtz free energies of interactions for protein-ligand atom pairs (Potential of Mean Force, PMF)
[f] G-score showing hydrogen bonding, complex (ligand-protein), and internal (ligand-ligand) energies.
[g] Chem-score points for H-bonding, lipophilic contact, and rotational entropy, along with an intercept term

interactions at the active site of the enzyme (PDB ID: 1JIJ). Among those, one interaction was from oxygen atom of 1,3,4-oxadiazole with hydrogen of LYS84 (O------H-LYS84, 2.04 Å), and second hydrogen bond interaction was raised from the N_1 nitrogen of 1,2,4-triazole ring with hydrogen atom of TYR170 (N-----H-TYR170, 2.49 Å).

Fig. 6 portrays the compound **9u** making seven hydrogen bonding interactions at the active site of the *S. aureus TyrRS* in complex with SB-239629 (PDB ID: 1JIJ). Among those
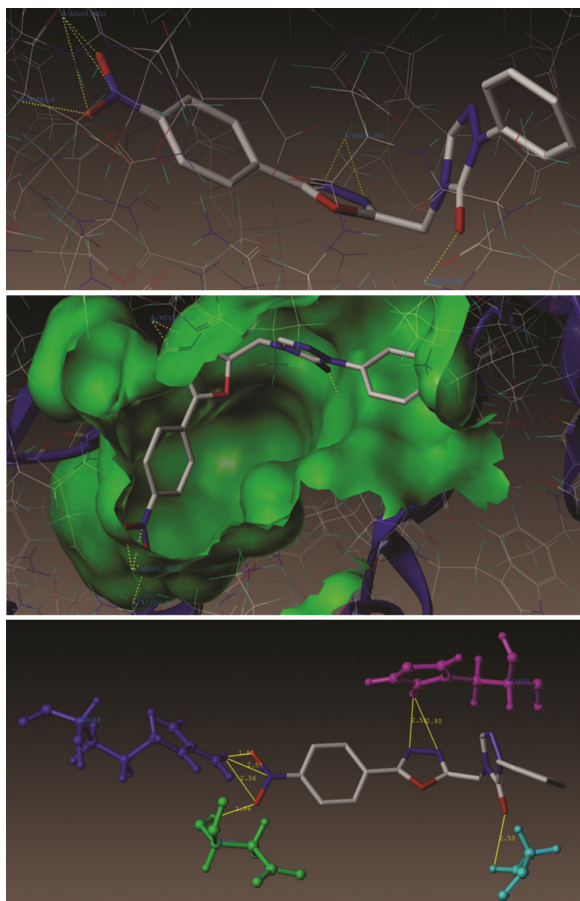

Fig. 6 — Docked view of compound **9u** at the active site of the enzyme PDB: 1JIJ

i) Three interactions were of oxygen atoms of nitro group present on the phenyl ring with hydrogen atoms of ASP80 and ARG88 (O------H-ASP80, 1.96 Å; O------H-ARG88, 2.56 Å; 1.90 Å).

ii) Nitrogen atoms present at the 3rd and 4th positions of 1,3,4-oxadiazle ring makes interactions with the hydrogen atom of HIS50 (N-----H-HIS50, 2.80 Å; 2.55 Å), oxygen atom present on the 3rd position of 1,2,4-triazole ring makes interaction with the hydrogen atom of GLY193 (O-----H-GLY193, 2.50 Å) and remaining another hydrogen bonding interaction raised from the nitrogen atom of nitro group present on the phenyl ring with hydrogen atom of ARG88 (N-----H-ARG88, 2.55 Å).

Fig. 7 represented the hydrophobic and hydrophilic amino acids surrounded to the compounds **9u** and **7m**. The binding interaction of Tetracycline with enzyme active sites showed 05 bonding interactions and the docked view of the same has been depicted in Fig. 8. All the compounds **7g-p** and **9t-y** along with the ligand were docked into the active site of enzyme as shown in Fig. S18. All the compounds showed consensus score in the range 4.63-6.03 indicating the summary of all forces of interaction between ligands and the enzyme and also it was observed that the studied compounds have demonstrated the similar interactions with amino acid residues (HIS50 and LYS84) as that of standard Tetracycline. This indicates that molecules preferentially bind to enzyme in comparison to the standard Tetracycline (Table 1).

Docking against lanosterol 14α-demethylase (CYP51) in complex with inhibitor Fluconazole (PDB ID: 3KHM)

The crystal structure of lanosterol 14α-demethylase (CYP51) in complex with inhibitor Fluconazole (PDB ID 3KHM, 2.85 Å X-ray diffraction) was extracted from the Brookhaven Protein Database (PDB http://www.rcsb.org/pdb)[20].

Anti-fungal activity investigation and detailed intermolecular interactions between the synthesized
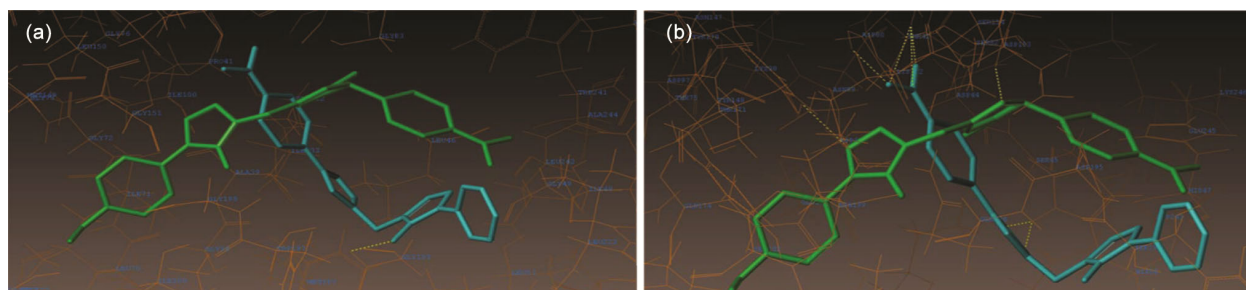

Fig. 7 — (a) Hydrophobic and (b) hydrophilic amino acids surrounded to compounds **9u** (green colour) and **7m** (cyan colour)
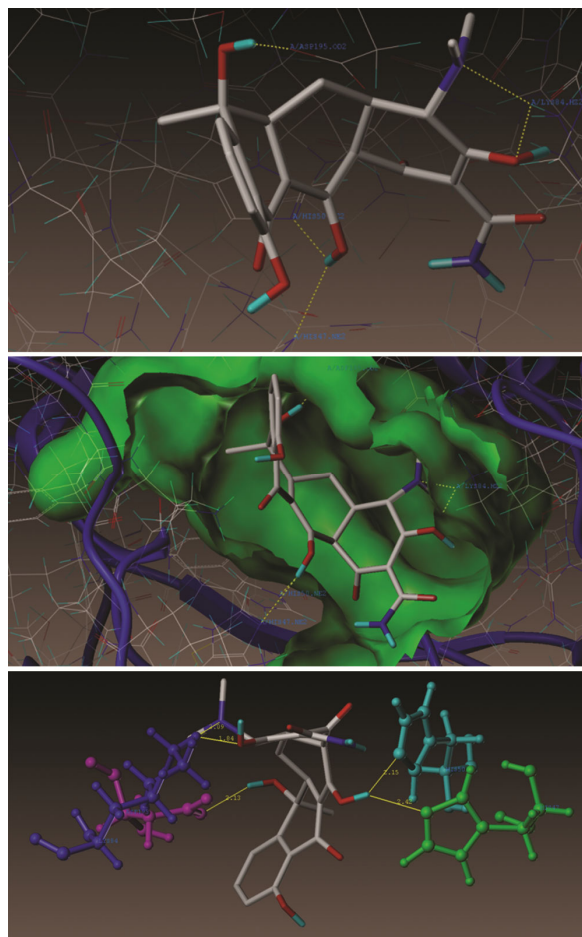
Fig. 8 — Docked view of Tetracycline at the active site of the enzyme PDB: 1JIJ

Fig. 9 — Docked view of compound **7j** at the active site of the enzyme PDB : 3KHM

compounds **7g-p** and **9t-y** were analyzed by molecular docking studies on the crystal structure of *lanosterol 14 α-demethylase* (CYP51) in complex with inhibitor Fluconazole [22] using the Surflex-dock programme of sybyl-X 2.0 software. As depicted in Fig. 9, compound **7j** makes three hydrogen bonding interactions at the active site of the enzyme (PDB ID: 3KHM). Among those an interaction was of oxygen atom of acetyl group present on the 4ᵗʰ position of 1,3,4-oxadiazole ring with hydrogen of TYR116 (O------H-TYR116, 2.68 Å), oxygen atom present on the 3ʳᵈ position of 1,2,4-triazole ring making an interaction with the hydrogen atom of TYR116 (O-----H-TYR116, 1.86 Å) and the remaining hydrogen bonding interaction was raised from the fluorine atom on the phenyl ring with hydrogen of ALA288 (F-----H-ALA288, 2.61 Å).

Fig. 10 shows compound **9u** forming three hydrogen bonding interactions at the active site of the enzyme (PDB ID: 3KHM), among those two

interactions were of oxygen atoms of nitro group present on the phenyl ring with hydrogen atoms of TYR116 (O------H-TYR116, 2.31 Å; 2.52 Å), and the remaining hydrogen bonding interaction was raised from the nitrogen atom of nitro group with hydrogen of TYR116 (N-----H-TYR116, 2.85 Å). Fig. 11 represents the hydrophobic and hydrophilic amino acids surrounded to the studied compound **9u** and **7j**. The binding interaction of Fluconazole with enzyme active sites shows three bonding interactions and the docked view of the same has been depicted in Fig. 12.

All the title compounds along with the ligand were docked into the active site of enzyme as shown in Fig. S19. The predicted binding energies of the compounds are listed in Table 2. The docking study revealed that all the compounds have shown very good docking score against the enzyme. All the compounds showed consensus score in the range

4.98 - 8.05, indicating the summary of all the forces of interaction between ligands and the enzyme and also it was observed that these compounds showed agnate interactions with amino acid residue (TYR116) as that of reference Fluconazole. This indicates that the title compounds preferentially bind to enzyme in a similar way to the reference Fluconazole.

In silico **pharmacokinetic assessment**

To avoid late stage failure for an orally administered drug, pharmacokinetic study forms an important tool. In the present report, the title compounds were subjected to pharmacokinetic

parameters obtained by Osiris Property Explorer [23], Pro-Tox II (Prediction of Toxicity of Chemicals) [22, 24], *Molinspiration softwares* [25] and the data obtained are presented in Table 3 and Table 4. The values of physicochemical prarameters such as molecular weight, hydrogen bond acceptors, hydrogen bond donors, CLogP, topological polar surface area, LogS, volume, druglikeliness and hence the effective drug score for both the set of the compounds *viz*., **7g-p** and **9t-y** and the standard drugs Tetracycline and Fluconazole are presented in Table 3. *LogP* the logarithm of its partition coefficient between
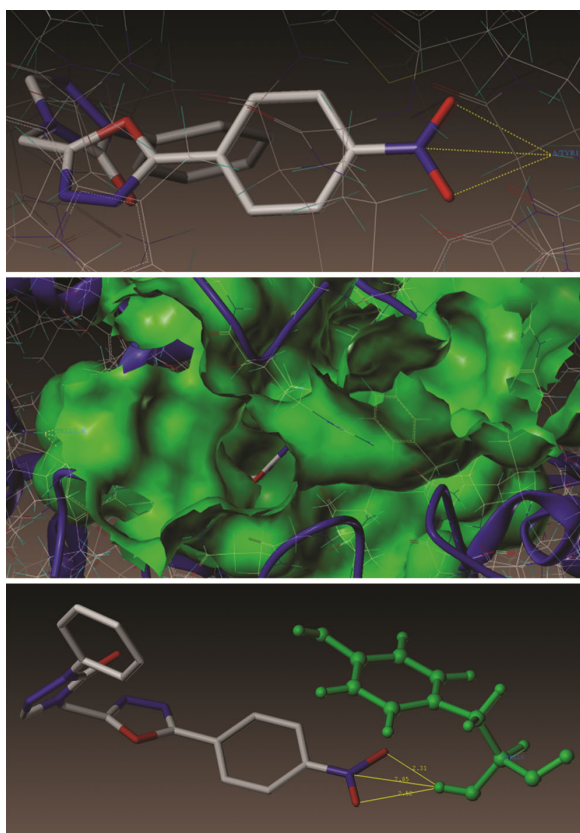

Fig. 10 — Docked view of compound **9u** at the active site of the enzyme PDB: 3KHM
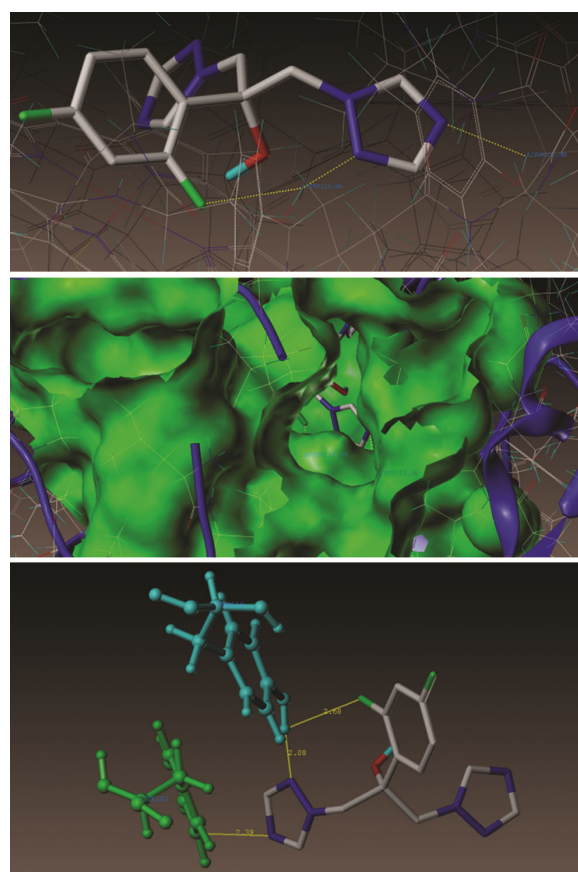

Fig. 12 — Docked view of Fluconazole at the active site of the enzyme PDB: 3KHM
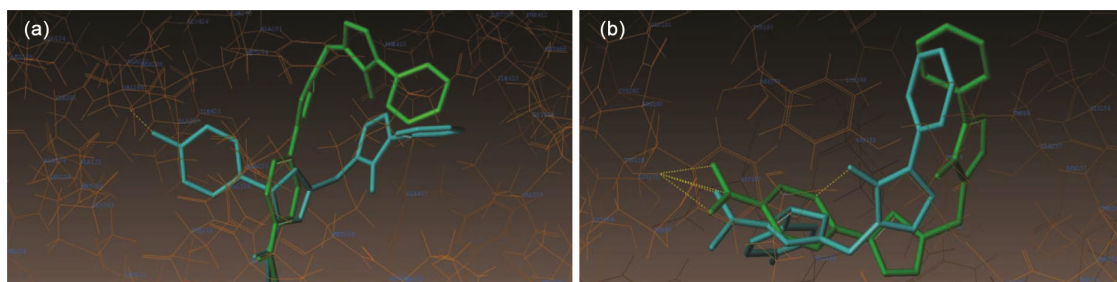

Fig. 11 — a) Hydrophobic and (b) hydrophilic amino acids surrounded to compounds **9u** (green color) and **7j** (cyan color)

Table 2 — Surflex Docking score (kcal/mol) of the title compounds **7g-p** and **9t-y** 14 α-demethylase (CYP51) in complex with inhibitor Fluconazole (PDB ID: 3KHM)

Entry No.	C Score[a]	Crash Score[b]	Polar Score[c]	D Score[d]	PMF Score[e]	G Score[f]	Chem Score[g]
7g	4.98	-2.97	2.70	-125.70	-129.92	-229.30	-34.01
7h	6.36	-0.75	3.39	-128.20	-84.55	-193.67	-28.46
7i	6.44	-1.92	2.39	-137.40	-134.35	-230.49	-35.89
7j	5.36	-3.61	1.23	-145.65	-98.72	-249.43	-31.44
7k	6.85	-0.89	0.00	-125.80	-68.66	-243.92	-24.92
7l	8.05	-1.37	2.26	-148.70	-131.60	-234.80	-33.52
7m	5.56	-1.71	0.00	-148.68	-108.14	-261.46	-27.45
7n	5.47	-2.73	2.55	-137.83	-128.47	-249.72	-36.50
7o	7.40	-2.48	2.35	-146.10	-128.77	-267.01	-34.83
7p	5.87	-1.62	0.00	-134.14	-69.99	-245.07	-25.83
9t	5.36	-2.36	1.29	-103.90	-92.68	-202.02	-26.94
9u	7.94	-3.60	2.48	-126.52	-84.15	-259.55	-27.88
9v	6.22	-2.73	1.99	-117.85	-80.91	-243.04	-31.37
9w	6.58	-1.82	0.94	-115.14	-103.03	-221.89	-27.24
9x	6.99	-0.98	3.44	-121.90	-78.37	-207.14	-27.86
9y	6.17	-4.35	2.42	-131.22	-87.47	-253.55	-34.67
Fluconazole	6.78	-1.16	3.25	-72.30	-152.70	-193.47	-22.37

[a]CScore (Consensus Score) integrates a number of popular scoring functions for ranking the affinity of ligands bound to the active site of a receptor and reports the output of total score.
[b]Crash-score revealing the inappropriate penetration into the binding site. Crash scores close to 0 are favorable. Negative numbers indicate penetration
[c]Polar indicating the contribution of the polar interactions to the total score. The polar score may be useful for excluding docking results that make no hydrogen bonds
[d]D-score for charge and van der Waals interactions between the protein and the ligand. [e]PMF-score indicating the Helmholtz free energies of interactions for protein-ligand atom pairs (Potential of Mean Force, PMF)
[f]G-score showing hydrogen bonding, complex (ligand-protein), and internal (ligand-ligand) energies
[g]Chem-score points for H-bonding, lipophilic contact, and rotational entropy, along with an intercept term

Table 3 — Evaluation of pharmacokinetic parameters of the target compounds **7g-p** and **9t-y**

Entry No.	MW	HBA	HBD	logP	TPSA (A^2)	LogS (mol/L)	Volume	Drug likeliness	Drug Score
7g	363.37	8	0	2.13	77.81	-3.48	315.78	6.0	0.71
7h	408.37	11	0	1.21	123.63	-3.94	339.12	-4.27	0.44
7i	397.82	8	0	2.73	77.81	-4.22	329.32	7.42	0.84
7j	381.37	8	0	2.23	77.81	-3.80	320.71	4.98	0.87
7k	393.40	9	0	2.06	87.04	-3.50	341.33	3.34	0.85
7l	393.40	9	0	2.06	87.04	-3.50	341.33	4.07	0.69
7m	438.40	12	0	1.14	132.86	-3.96	364.66	-6.21	0.42
7n	427.85	9	0	2.66	87.04	-4.24	354.87	5.48	0.81
7o	411.39	9	9	2.16	87.04	-3.82	346.26	3.03	0.83
7p	423.43	10	0	1.99	96.27	-3.52	368.88	1.28	0.75
9t	319.32	7	0	2.73	74.83	-4.45	273.89	5.68	0.90
9u	364.32	10	0	2.79	120.6	-4.91	297.22	-6.01	0.45
9v	383.84	7	0	4.31	74.83	-5.19	287.42	5.53	0.85
9w	349.35	8	0	2.66	84.06	-4.47	299.43	3.69	0.88
9x	394.35	11	0	1.74	129.88	-4.93	322.77	-8.24	0.44
9y	383.79	8	0	3.27	84.06	-5.21	312.97	3.55	0.82
TCN	426.46	9	5	-0.18	161.39	-2.46	369.75	5.74	0.83
FCZ	310.30	7	1	-0.11	81.65	-2.17	240.96	1.99	0.90

n-octanol and water log($c_{octanol}/c_{water}$), is a well established measure of the compound's hydrophilicity. Low hydrophilicities and therefore high *logP* values cause poor absorption or permeation.

It has been shown for the compounds to have a reasonable probability of being well absorbed if their *logP* values are less than 5.0 and interestingly all the title compounds have the *logP* values less than 5 thus

showing hydrophilicity and hence optimum permeation of the all these title compounds.

A lead molecule can be an effective drug if it has the predicted water solubility range (logS) which lies in between 0.5-6.50 (mol/L). Interestingly, all the reported molecules have low logS values. The polar surface area (TPSA) of these compounds including the standard was less than 140ºA^2. It was observed from the above study that the newly synthesized compounds followed RO5 (Rule of Five), representing more drug-like nature and drug score. It may also be emphasized that the compounds **9t-y** exhibited impressive drug score than the compounds **7g-p**.

Toxicity analyses

Newer molecules need to go through the toxicity analyses during drug design and development. Computational toxicity study is not only a rapid test to determine the toxic doses in animals, it can also facilitate to minimize the animal experiments. Protox [26] estimates rodent oral toxicity, which is assessed from compounds of known drug candidates and their toxicity by their toxic fragments or chemical structure. Protox gives a comparative account of the similarity of structures of synthesized molecules which will be loaded in a server with information of molecules having antecedently proverbial toxicity and identifies the toxic fragments of loaded molecules and probable toxicity targets. Toxic doses are often known as LD50 values in mg per kg body weight. The LD50 is the median lethal dose, meaning the dose at which 50% of test subjects die upon exposure to a compound. The predicted LD50 for our target molecules is above 300 mg/kg and less than 2500 mg/kg for all the tested compounds as shown in Table 4. Only the compound **7h** has shown moderate carcinogenicity and mutagenicity where as **7g**, **7m**, **9t**, **9u**, **9w** and **9x** have shown mild carcinogenicity. The compounds **7g**, **7l** and **9u** have also exhibited mild mutagenicity. It is a salient observation that no compound has exhibited immunogenic, cyotoxic and tumorogenic effect. However, all the title compounds **7g-p** and **9t-y** including the standard drugs Tetracycline and Fluconazole are mild hepatotoxic. Nevertheless, it is interesting to note that these newly synthesized molecules **7g-p** and **9t-y** come under the toxicity category of Class 4 (harmful only if administered (300 < LDS50 ≤ 2000 mg/kg) except **9u** and **9x** which belong Class 5 (may be harmful if swallowed (2000 < LDS50 ≤ 5000 mg/kg). The standard antibacterial Tetracycline and antifungal

Fluconazole belong to the Class 4 toxicity category. Hence, careful maintenance of the dose will prove these molecules as useful pharmacological agents. Also, there are no toxic fragments present as claimed by the developer's limits. This toxicity prediction study reviews that synthesized molecules can be the lead molecules for further analysis.

Antimicrobial activity assay

In order to evaluate the antimicrobial susceptibility of the synthesized compounds, NCCLS (National Committee on Clinical Laboratory Standards) macro-dilution broth method was carried out. The minimum inhibitory concentration (MIC) value was determined as the lowest concentration of the synthesized compounds that inhibited the growth of the test microorganisms. Various concentrations of samples were added to the respective tube to carry out NCCLS macro dilution broth method [27].

Antibacterial activity

Different concentrations (0.125-256 µg/mL) of the synthesized compounds **7g-p** and **9t-y** were added to the respectively labelled sterile Mueller Hinton Broth (MHB) medium tubes. The tubes were inoculated with lag phase cultures (1.00 mL) of the Gram positive bacteria *S. aureus* and *B. subtilis*, and that of the gram negative bacteria *E. coli* and *P. aeruginosa*. The inoculated tubes were incubated at 37 ºC for 24 h followed by observing the inhibition of growth of the test bacteria in the tubes. The MIC was determined as the lowest concentration of the synthesized compounds **7g-p** and **9t-y** containing tube showing no visible growth of the test bacteria.

Antifungal activity

Different concentrations (0.125-256 µg/mL) of the synthesized compounds **7g-p** and **9t-y** were added to the respectively labeled sterile Saboraud dextrose broth tubes. The tubes were inoculated with lag phase cultures of the fungi *A. niger*, *A. flavus, A. fumigatus, T. atroviridae, T. harzianum, P. chrysogenum, P. citranum* and *C. albicans*. The inoculated tubes were incubated at 27 ºC for 48 h followed by observing the Inhibition of growth of the test fungi in the tubes. The MIC was determined as the lowest concentration of the title compounds containing tube showing no visible growth of the test fungi.

Results of *in vitro* antibacterial activity

The newly synthesized compounds **7g-p** and **9t-y** were evaluated for their antibacterial activity against

two Gram-positive (*S. aureus and B. subtilis*) and two Gram-negative (*E. coli and P. aeruginosa*) bacterial strains with Tetracycline as a standard drug. The minimum inhibitory concentrations (MIC) for 1,2,4-triazole clubbed 1,3,4-oxadiazoles were observed in the range of 0.125-128 µg/mL. The MIC of the synthesized molecules was compared with Tetracycline. It was disclosed that all of the new compounds showed variable degrees of inhibition against the tested microorganisms. The preliminary antibacterial activity revealed that most of the molecules possess excellent activity against each Gram positive and Gram negative microorganism strains. In general, more selective inhibitory activity against Gram positive *S. aureus* and Gram negative *E. coli* bacterial strains. The MIC results obtained are represented in Table 5.

Table 4 — Oral Toxicity prediction results of the compounds **7g-p** and **9t-y**

Entry No.	Toxicity Effects					Organ Toxicity	Predicted LD50	Predicted Toxicity Class
	Carcino	Immuno	Mutagen	Cyto	Tumorogen	Hepato	(mg/kg)	
7g	+	-	+	-	-	+	1190	4
7h	++	-	++	-	-	+	1000	4
7i	-	-	-	-	-	+	1000	4
7j	-	-	-	-	-	+	1000	4
7k	-	-	-	-	-	+	1000	4
7l	-	-	+	-	-	+	1000	4
7m	+	-	-	-	-	+	1000	4
7n	-	-	-	-	-	+	1000	4
7o	-	-	-	-	-	+	1000	4
7p	-	-	-	-	-	+	1000	4
9t	+	-	-	-	-	+	2000	4
9u	+	-	+	-	-	+	453	5
9v	-	-	-	-	-	+	453	4
9w	+	-	-	-	-	+	1600	4
9x	+	-	-	-	-	+	2500	5
9y	-	-	-	-	-	+	1600	4
TCN	-	+	-	-	-	+	1007	4
FCZ	-	-	-	-	-	+	1200	4

Class 1: Fatal if swallowed (LDS50 < 5mg/kg), Class 2: Fatal if swallowed (5 < LDS50 ≤ 50 mg/kg), Class 3: Fatal if swallowed (50 < LDS50 ≤ 300 mg/kg), Class 4: Harmful if swallowed (300 < LDS50 ≤ 2000 mg/kg), Class 5: May be harmful if swallowed (2000 < LDS50 ≤ 5000 mg/kg), Class 6: Non Toxic (LDS50 > 5000 mg/kg), TCN: Tetracycline, FCZ: Fluconazole.

Table 5 — *In vitro* antibacterial activity data of compounds **7g-p** and **9t-y** (MIC µg/ml)

Entry No	Gram +ve bacteria		Gram –ve bacteria	
	S. aureus	*B. subtilis*	*E. coli*	*P. aeruginosa*
7g	32	64	64	128
7h	0.12	0.5	0.5	0.5
7i	2.0	2.0	1.0	1.0
7j	2.0	2.0	0.5	1.0
7k	4.0	8.0	2.0	4.0
7l	4.0	8.0	8.0	16
7m	1.0	0.5	2.0	2.0
7n	2.0	1.0	2.0	2.0
7o	4.0	2.0	2.0	4.0
7p	32	64	16	64
9t	8.0	4.0	8.0	16
9u	1.0	1.0	0.5	0.12
9v	0.5	0.5	2.0	2.0
9w	4.0	2.0	2.0	2.0
9x	16	32	8.0	16
9y	8.0	16	4.0	8.0
Tetracycline	0.5	0.25	0.5	0.5

Table 6 — *In vitro* antifungal activity (MIC µg/ml) of the target compounds 7g-p and 9t-y

Entry No.	*A. niger*	*A. flavus*	*A. fumigatus*	*T. atroviridae*	*T. harzianum*	*P. chrysogenum*	*P. citranum*	*C. albicans*
7g	128	128	128	64	64	64	64	16
7h	1.0	1.0	1.0	0.5	0.5	0.5	0.5	0.25
7i	2.0	2.0	2.0	1.0	1.0	1.0	1.0	4.0
7j	4.0	4.0	4.0	2.0	2.0	2.0	2.0	2.0
7k	8.0	8.0	4.0	4.0	8.0	4.0	4.0	1.0
7l	16	16	16	8.0	8.0	8.0	8.0	4.0
7m	64	64	64	32	32	32	32	16
7n	8.0	8.0	8.0	4.0	4.0	4.0	4.0	2.0
7o	8.0	8.0	8.0	8.0	8.0	8.0	8.0	4.0
7p	32	32	32	16	16	16	16	4
9t	16	16	16	8.0	8.0	8.0	8.0	2.0
9u	2.0	4.0	1.0	1.0	1.0	1.0	2.0	1.0
9v	8.0	8.0	4.0	4.0	2.0	2.0	2.0	2.0
9w	8.0	8.0	8.0	8.0	4.0	4.0	4.0	8.0
9x	16	32	16	32	32	32	16	16
9y	8.0	4.0	16	33	16	16	8.0	8.0
Fluco-nazole	1.0	0.5	1.0	1.0	1.0	0.5	1.0	2.0

Compounds **7h**, **7i**, **7j**, **9u**, and **9v** exhibited excellent antibacterial inhibitions against both Gram-positive and Gram-negative bacteria. The compounds **7m**, **7n** and **7o** have shown good inhibition and the remaining compounds displayed moderate activity against both bacterial strains. The compounds having *chloro*, *fluoro* and *nitro* substituent on the phenyl ring exhibited higher activity than those with *methoxy* substituents. The presence of electronegative atom *viz., nitro* and *chloro* in the aromatic ring system may enhance the biological potency, bioavailability, metabolic stability and lipophilicity. Enhanced lipophilicity may lead to easier absorption and transportation of molecules within the biological systems[28]. Generally, it was observed that electron withdrawing atoms/groups such as *fluoro*, *chloro* and *nitro* at the 4th position of the phenyl ring contributed to *in vitro* results in case of antibacterial activity, whereas *methoxy* has lesser inhibition. Especially *nitro* group at the 4th position is responsible for the enhancement in *in vitro* activity. The increase in activity with respect to the substituent follows the order as, $NO_2 > F > Cl > OCH_3 > H$ [29]. The other comparative study between two series represents that the presence of acetyl group on nitrogen atom of the 1,3,4-oxadiazole enhanced the *in-vitro* biological activity.

Results of antifungal activity

The *in vitro* antifungal activity of newly synthesized compounds **7g-p** and **9t-y** were screened against eight different human pathogenic fungi by using micro dilution broth method. The MIC values of all tested compounds in comparison with standard Fluconazole is displayed in Table 6.

Compounds **7g**, **7h**, **7i** and **9u** exhibited excellent antifungal activity against all pathogenic fungal strains with lower MIC value range 0.50 - 4.00 µg/mL. Remaining molecules displayed moderate to good antifungal activity. Introduction of acetyl group on nitrogen enhances the in-vitro activity. The compounds containing more electro negative groups *viz.*, *nitro*, *chloro* and *fluoro* exhibited potent biological activity follows the order as $NO_2 > F > Cl > OCH_3 > H$. Thus, these molecules may be considered as lead molecules to explore the activity against fungi.

Conclusion

1,2,4-Triazole and 1,3,4-oxadiazoles are important structural moieties of many pharmaceutical drugs. In view of this, 1,2,4-triazole obtained using N-arylsydnone as synthon was appended to the 1,3,4-oxadiazole to obtain the title compounds **7g-p** and **9t-y**. These previously unknown molecules were subjected to Docking analysis against *S. aureus tyrosyl-tRNA synthetase* (PDB: 1JIJ) and *lanosterol-14α-demethylase* complex with standard inhibitor Fluoconazole (PDB: 3KHM) anticipating their antibacterial and antifungal activity. Further, these molecules were analyzed for their toxicity, drug-likeness and drug score. All of the molecules have shown the least toxicity and also the *in vitro* antimicrobial inhibition results of these compounds are excellent thus propelling these lead molecules for the future pharmacologically important scaffolds.

Supplementary Information

Supplementary information is available in the website http://nopr.niscpr.res.in/handle/123456789/58776.

References

1   Boyer J H, *In Heterocyclic Compounds, Ed R C Elderfield* (John Wiley & Sons Inc, New York) 1961, 463.

2   Oliveira C S D, Lira B F, Barbosa-Filho J M, Lorenzo J G F & Athayde-Filho P F D, *Molecules,* 17 (2012) 10192.

3   Patel K D, Prajapati S M, Panchal S N & Patel H D, *Synth Commun*, 44 (2014) 1859.

4   (a) Rajak H, Agarawal A, Parmar P, Thakur B S, Veerasamy R, Sharma P C & Kharya M D, *Bioorg Med Chem Lett*, 21 (2011) 5735; (b) Ahsan M J, Bhandari L, Makkar S, Singh R, Hassan M Z, Geesi M H, Jadav B M A, S S, Balaraju T, Riadi Y, Rani S, Khalilullah H, Gorantla V & Hussain A, *Lett Drug Des Dis*, 17 (2020) 145.

5   Ramankutty B C, Ilango K, Prathap M & K R, *J Young Pharm*, 4 (2012) 33.

6   Gan X, Hu D, Li P, Wu J, Chen X, Xue W & Song B, *P Manag Sci*, 72 (2016) 534.

7   (a) Yatam S, Jadav S S, Gundla R, Gundla K P, Reddy G M, Ahsan M J & Chimakurthy J, *ChemistrySelect*, 3 (2018) 10305; (b) Rathore A, Sudhakar R, Ahsan M J, Ali A, Subbarao N, Jadav S S, Umar S & Yar M S, *Bioorg Chem*, 70 (2017) 107.

8   Ahsan M J, Sharma J, Singh M, Jadav S S & Yasmin S, *Bio Med Res Int,* (Hindawi) 2014, pp. 1.

9   Ahsan M J, Sharma J, Bhatia S, Kumar Goyal P, Shankhala K & Didel M, *Lett Drug Des Dis*, 11 (2014) 413.

10   Singh R & Chauhan A, *Intl J Adv Biol Res*, 3 (2013) 140.

11   Sudeesh K & Gururaja R, *Org Chem Curr Res*, 6 (2017) 2.

12   Nimavat B, Mohan S, Saravanan J, Deka S, Talukdar A, Sahariah B J, Dey BK & Sharma R K, *Int J Res Pharm Chem*, 2 (2012) 594.

13   (a) Shiradkar M R, Murahari K K, Gangadasu H R, Suresh T, Kalyan C A, Panchal D, Kaur R, Burange P, Ghogare J, Mokale V & Raut M, *Bioorg Med Chem*, 15(2007) 3997; (b) Thompson G R, Cadena J & Patterson T F, *Clin Chest Med*, 30 (2009) 203.

14   Ram V J, Sethi A, Nath M & Pratap R, *The Chemistry of Heterocycles- Nomenclature and Chemistry of three to five Membered Heterocycles* (Elsevier, Netherland) 2019, 149.

15   (a) Somagond S M, Kamble R R, Kattimani P P, Shaikh S K J, Dixit S R, Joshi S D & Devarajegowda H C, *Chemistry Select*, 3 (2018) 2004; (b) Cherepanov I A & Moiseev S K, *Advances in Heterocyclic Chemistry, Recent Developments in the Chemistry of Sydnones and Sydnone imines* (Elsevier, Netherland) 2020, pp. 49.

16   Zhu-Ping X, Tao-Wu M, Mei-Lin L, Yu-Ting F, Xiao-Chun P, Jia-Liang L, Zhi-Ping L, Ying W, Qun L, Yang D, Xiao L & Hai-Liang Z, *Eur J Med Chem*, 46 (2011) 4904.

17   Bouchal B, Farid A, Takfaoui A, Errahhali M E, Errahhali M E, Dixneuf P H , Doucet H, Touzani R & Bellaoui M, *BMC Chemistry*, 13 (2019) 100.

18   (a) Kattimani P P, Kamble R R, Dorababu A, Hunnur R K, Kamble A A & Devarajegowda H C, *J Heterocyl Chem,* 54 (2017) 2258; (b) Somagond S M, Kamble R R, Shaikh S K J, Bayannavar P K & Joshi S D, *ChemistrySelect,* 3 (2018) 8529; (c) Sybyl-X Molecular Modeling Software Packages, Version 2.0 TRIPOSE Associates Inc (2012) St. Louis, MO, USA, http://sybyl-x.software.informer.com/2.0/.

19   Patel N B & Khan I H, *J Enzyme Inhib Med Chem,* 26 (2011) 527.

20   (a) Pagdala N S, Syed K & Tuszynski J, *Biophys Rev*, 9 (2017) 91; (b) Gasteiger J & Marsili M, *Tetrahedron*, 36 (1980) 3219; (c) Tripos International, Sybyl-X 2.0, Tripos International, St. Louis, MO, USA (2012).

21   Xiao Z-P, Ma T-W, Liao M-L, Feng Y-T, Peng X-C, Li J-L, Li Z P, Wu Y, Luo Q, Deng Y, Liang X & Zhu H L, *Eur J Med Chem,* 46 (2011) 4904.

22   Somagond S M, Kamble R R, Bayannavar P K, Shaikh S J, Joshi S D, Kumbar V M, Nesaragi A R & Kariduraganavar M Y, *Archive Der Pharmazie*, 352 (2019) 1900013.

23   (a) Ayati A, Falahati M, Irannejad H & Emami S, *Daru,,* 20 (2012) 46; (b) Organic Chemistry Portal 2012, http://www. organic-chemistry.org/prog/peo/ Accessed on March 15, 2021.

24   (a) Banerjee P, Eckert A O, Schrey A K & Preissner R, *Nucleic Acids Research*, 46 (2018) 257; (b) http://tox-newcharite.de/protox_II.

25   (a) Khan T, Dixit S, Ahmad R, Raza S, Azad I, Joshi S & Khan A R, *J Chem Biol,* 10 (2017) 91; (b) Mabkhot Y N, Alatibi F, El-Sayed N N E, Al-Showiman S, Kheder N A, Wadood A, Rauf A, Bawazeer S & Hadda T B, *Molecules, 21 (*2016) 222; (c) https://www.molinspiration.com/cgi-bin/properties.

26   Dutta S K, Basu S K & Sen K K, *J Expt Biol,* 44 (2006) 123.

27   Julia A K, George E H, Max S, Wendy A, Catherine M & Cynthia Carlyn, *J Clinical Microbilol*, 38 (2000) 3341.

28   (a) Di L & Kerns E H, *In Drug-Like Properties* (Elsevier, Netherland) 2016, 39; (b) Tomasz P, Wujec M, Kosikowska U & Malm A, *Lett Drug Des Discov*, 10 (2013) 492, (c) De-Almeida C G, Garbois G D, Amaral L M, Diniz C C & Hyaric M L, *Biomed Pharmacother*, 64 (2010) 287.

29   Peterson L R, *Clin Infect Dis,* 33 (2001) 180.